JACS
JOURNAL OF THE AMERICAN CHEMICAL SOCIETY

Article

pubs.acs.org/JACS

Fluorogenic Ubiquinone Analogue for Monitoring Chemical and Biological Redox Processes

Lana E. Greene, Robert Godin, and Gonzalo Cosa*

Department of Chemistry and Center for Self Assembled Chemical Structures (CSACS/CRMAA), McGill University, 801 Sherbrooke Street West, Montreal, Quebec H3G 0B8, Canada

Supporting Information

ABSTRACT: We report herein the synthesis and characterization of a fluorogenic analogue of ubiquinone designed to reversibly report on redox reactions in biological systems. The analogue, **H_2B-Q**, consists of the redox-active quinone segment found in ubiquinone, 2,3-dimethoxy-1,4-benzoquinone, coupled to a boron-dipyrromethene (BODIPY) fluorophore segment that both imparts lipophilicity in lieu of the isoprenyl tail of ubiquinone, and reports on redox changes at the quinone/quinol segment. Redox sensing is mediated by a photoinduced electron transfer intramolecular switch. In its reduced dihydroquinone form, **H_2B-QH$_2$** is highly emissive in nonpolar media (quantum yields 55−66%), while once oxidized, the resulting quinone **H_2B-Q** emission is suppressed. Cyclic voltammetry of **H_2B-Q** shows two reversible, 1-electron reduction peaks at −1.05 V and −1.37 V (vs ferrocene) on par with those of ubiquinone. Chemical reduction of **H_2B-Q** by $NaBH_4$ resulted in >200 fold emission enhancement. **H_2B-QH$_2$** is shown to react with peroxyl radicals, a form of reactive oxygen species (ROS) as well as to cooperatively interact with chromanol (the active segment of α-tocopherol). Kinetic analysis further shows the antioxidant reactivity of the nonfluorescent intermediate semiquinone. We anticipate that the **H_2B-Q/H_2B-QH$_2$** off/on reversible couple may serve as a tool to monitor chemical redox processes in real-time and in a noninvasive manner.

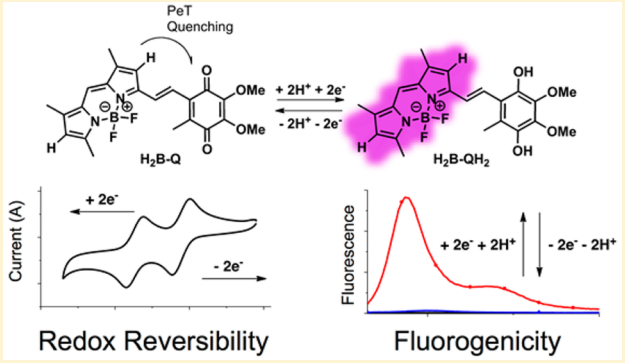

INTRODUCTION

The mitochondrion is the major production site of cellular energy during aerobic respiration. Following electron transport in the electron transport chain of the inner mitochondrial membrane through a series of relay systems, electrons from, e.g., NADH and succinate are transferred to oxygen, reducing it to water, and releasing energy. This energy is next stored as a proton gradient and ultimately in the form of adenosine triphosphate (ATP).[1]

The essential cofactor ubiquinone (coenzyme Q10), situated in the hydrophobic core of the inner mitochondrial membrane lipid bilayer is actively involved in the transport of the electrons through the membrane. Due to its lipophilicity and its redox reversibility, ubiquinone may serve as both a mobile transporter of electrons in the redox reactions of the electron transport chain, and as a hydrogen carrier to create a proton gradient between the mitochondrial matrix and the mitochondrial intermembrane space.[2−4] Importantly, ubiquinone has three redox states: ubiquinone (oxidized), ubisemiquinone (1 electron reduction from ubiquinone to yield a semiquinone radical), and ubiquinol (2 electron reduced form). Various protonation states are also possible for the reduced species, leading to complex proton-coupled electron transfer processes.[5,6] Besides acting as a transporter of electrons and protons in the electron transport chain, ubiquinol is also involved in preventing lipid peroxidation within the mitochondrial membrane via trapping peroxyl radicals either by itself or via regenerating other antioxidants such as α-tocopherol (vitamin E).[7,8] The intermediate ubisemiquinone radical formed in these processes is however considered to promote oxidation through direct reaction with molecular oxygen to generate superoxide radical anion.[9]

Regular cell homeostasis is intrinsically associated with the chemical activity of ubiquinone in its triple role as an electron and proton couple transporter, and as an antioxidant. Not surprisingly, a number of pathologies are associated with ubiquinone deficiency.[10−15] Key to understanding the complex role of ubiquinone and its association to disease, as well as the palliative effect of new drugs, is the availability of probes with the proper chemical selectivity and enhanced sensitivity toward monitoring the complex redox pathways of quinones in biological systems real-time, in situ and in a nonperturbing manner.[16−18]

Here we describe the design, preparation, and characterization of a two-segment receptor−reporter[19] fluorogenic analogue of ubiquinone conceived to report on the redox status of cellular environments. The new probe was obtained

Received: July 4, 2016
Published: August 10, 2016

DOI: 10.1021/jacs.6b06899
J. Am. Chem. Soc. 2016, 138, 11327−11334

upon covalently binding 2,3-dimethoxy-1,4-benzoquinone, the redox-active quinone segment found in ubiquinone (receptor segment), to a lipophilic boron-dipyrromethene (BODIPY) fluorophore (reporter segment). The new compound exploits activation/deactivation of photoinduced electron transfer (PeT)[20] between the trap and reporter segments to switch off/on the emission from the BODIPY core yielding a highly sensitive probe of redox status. Cyclic voltammogram experiments conducted in organic solutions confirmed that the redox potentials for the quinone segment of the new probe are on par with those reported for ubiquinone. Redox chemical reactions conducted in bulk in the presence of reducing and oxidizing agents validated the fluorogenic character of the probe, its sensitivity to redox processes and its reversible nature. Experiments with both peroxyl radicals and a fluorogenic analogue of α-tocopherol previously reported by us (H_2B-PMHC)[21] confirmed that the quinol segment regenerates chromanol as well as competitively scavenges free radicals. The new probe, for which we have coined the name H_2B-Q, appropriately emulates the partitioning and reactivity of ubiquinone and displays desirable fluorescence sensitivity. We anticipate that H_2B-Q may serve as a tool to image redox processes, potentially including the cellular level, in real-time and in a noninvasive manner.

RESULTS AND DISCUSSION

Design. Our design incorporated 2,3-dimethoxy-1,4-benzoquinone, the active part of ubiquinone, as the redox-sensitive receptor segment to emulate both the redox properties and the antioxidant activity of the ubiquinone/ubiquinol redox couple. Our design further envisioned a BODIPY lipophilic fluorophore as a reporter segment in lieu of the isoprenoid tail of ubiquinone, to preserve in the new probe the preferential partitioning of ubiquinone within lipid membranes.[21,22] In addition to the desirable lipophilic character, BODIPY fluorophores have optimal spectroscopic properties and are easily modified synthetically to accommodate groups of interest.[23−25] Furthermore, the redox properties of BODIPY dyes can be tuned to facilitate exergonic PeT in order to impart a fluorescence "off/on" switching mechanism in the redox probe and ensure a high contrast between off (oxidized) and on (reduced) states.[21,26]

To calculate and visualize the HOMO, LUMO, HOMO−1 and LUMO+1 of the optimized geometries of H_2B-Q (oxidized) and H_2B-QH_2 (reduced), and to predict the potential for PeT, we employed density functional theory (DFT) calculations at the B3LYP 6-31G(d) level[27] (Figures S1, S2). Our results suggest an operating PeT mechanism for H_2B-Q but not for H_2B-QH_2 and was experimentally validated (see Spectroscopic Properties). Here the oxidized form (H_2B-Q) is quenched due to PeT from the photoexcited BODIPY to the LUMO of the quinone moiety (BODIPY photoinduced oxidation, Scheme 1). Reduction of the quinone to the dihydroquinone (H_2B-QH_2) deactivates PeT and restores emission by raising the HOMO and LUMO of the ubiquinol segment preventing efficient electron transfer from the BODIPY dye.

Synthesis. Our preparation involved a convergent synthesis where the BODIPY dye and a precursor of the redox active quinone segment were prepared separately and next coupled via Knoevenagel condensation. A BODIPY-phenol conjugate (H_2B-phenol) was thus initially prepared where the phenol segment carried a free *para* position that would next be oxidized to the desired quinone. This strategy circumvented the challenges associated with the synthesis and purification of dihydroquinones (prone to auto-oxidation) and quinones (Michael acceptors prone to nucleophilic attack).

Scheme 1. (A) Structure of Ubiquinone (B) Proposed Off/On Sensing Mechanism for H_2B-Q Relying on PeT

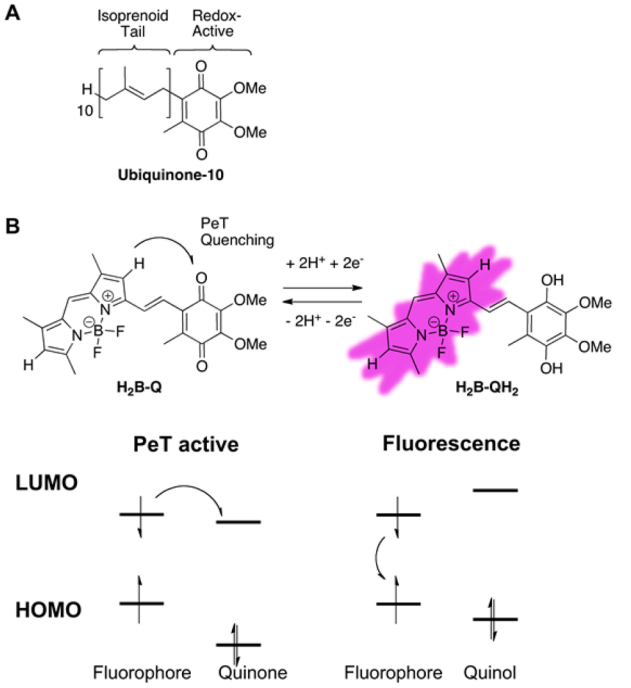

Compound **1** was chosen as our starting material for the synthesis of the precursor of the redox active quinone segment, where a formyl moiety was installed using the Vilsmeier−Haack reaction according to literature procedures (Scheme 2).[28] The methoxy group *ortho* to the formyl moiety was selectively demethylated using boron tribromide.[29,30] Removal of this methoxy group yielded compound **2** with the desired free phenol bearing a formyl moiety needed for coupling to BODIPY **5** via Knoevenagel condensation (vide infra). The BODIPY dye **5** was synthesized from **3** and **4** following the literature.[31]

In order to couple phenol **2** and BODIPY **5** we employed a Knoevenagel condensation[32] in the presence of 4-methylpiperidine and glacial acetic acid to give H_2B-phenol as a fluorescent dye. Subsequent oxidation of H_2B-phenol to give the corresponding nonfluorescent quinone (H_2B-Q) was performed using catalytic amounts of the cobalt catalyst salcomine. H_2B-Q was finally reduced to the corresponding dihydroquinone, H_2B-QH_2 through in situ production of hydrogen gas from cyclohexene in the presence of palladium catalyst.

Spectroscopic Properties. The absorption and fluorescence maxima, fluorescence quantum yields (ϕ_f), absorption extinction coefficients and fluorescence decay lifetimes (τ_{dec}) of H_2B-phenol, H_2B-Q, and H_2B-QH_2 are listed in Table 1. The dyes prepared here are characterized by red-shifted absorption (ca. 580 nm) compared to precursor **5**[31] (505 nm) due to the extended conjugation of the BODIPY resulting upon the Knoevenagel condensation which installs an arylvinyl moiety bond. H_2B-phenol and H_2B-QH_2 both exhibit a weak absorption band around 330 nm corresponding to the aryl group, while H_2B-Q exhibits a strong absorption band at 287

DOI: 10.1021/jacs.6b06899
J. Am. Chem. Soc. 2016, 138, 11327−11334

Scheme 2. Synthesis of H_2B-phenol, H_2B-Q, and H_2B-QH_2

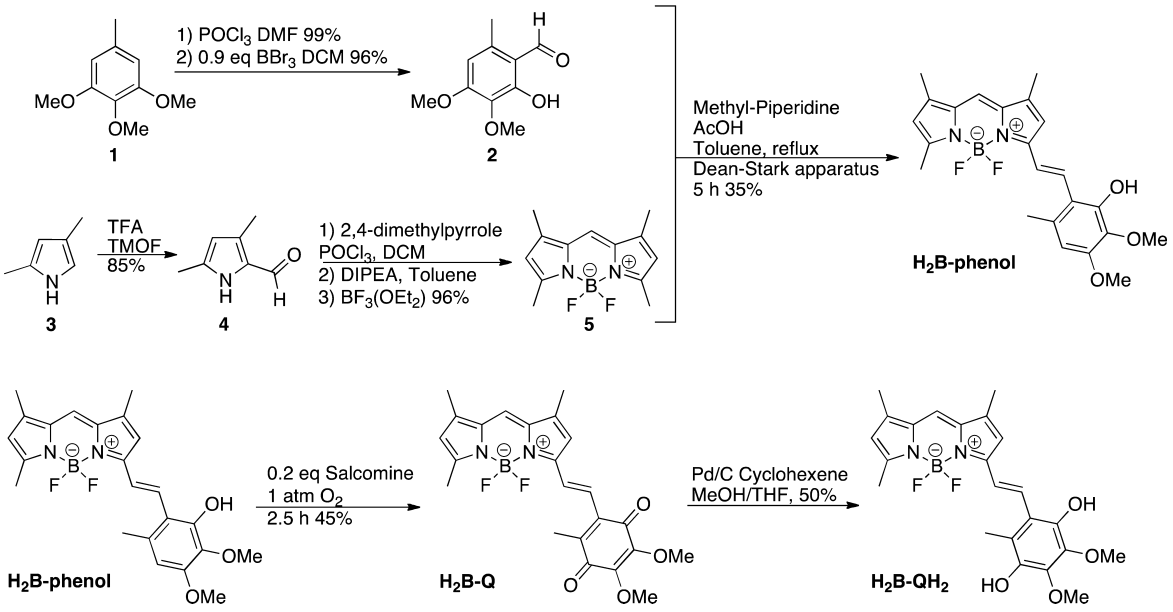

Table 1. Spectroscopic Properties of H_2B-phenol, H_2B-Q and H_2B-QH_2 in Various Solvents

dye	solvent	Abs λ_{max}	Em λ_{max}	ε x 10^3 (M^{-1} cm^{-1})	ϕ_f	τ_{dec} (ns)
H_2B-phenol	MeCN	574	602	91	0.65	3.84
	Toluene	584	597	95	0.88	3.67
	DCM	582	595	89	0.80	3.83
H_2B-Q	MeCN	573	N/A	35	<0.01	N/A
	Toluene	583	740[a]	37	0.02	0.37
	DCM	582	N/A	34	<0.01	N/A
H_2B-QH_2	MeCN	572	592	45	0.01	N/A
	Toluene	582	595	51	0.66	3.62
	DCM	579	595	41	0.55	3.16

[a]The significant differences in emission properties in toluene, namely a large Stokes shift, short lifetime, and solvent dependence, indicate a probable change in emission mechanism which we tentatively propose to be intramolecular charge transfer emission.[34]

nm corresponding to the quinone moiety (Figure S3), in line with previous optical investigation of ubiquinones.[33]

As predicted by the DFT calculations, **H_2B-Q** is nonemissive in polar (acetonitrile) and nonpolar (dicholormethane) solvents. **H_2B-phenol** is very fluorescent in all solvents studied, **H_2B-QH_2** is highly fluorescent in nonpolar solvents, with quantum yields ranging from 55%−66%. In polar solvents such as acetonitrile, however, the emission of **H_2B-QH_2** is reduced (quantum yield ∼1%). We postulate that PeT from the HOMO of the dihydroquinone moiety to the photoexcited BODIPY segment (BODIPY photoinduced reduction) readily occurs in polar solvents where charge transfer and formation of radical ions is stabilized. In summary, the oxidized form **H_2B-Q** is nonemissive, while, as per design, the reduced form **H_2B-QH_2** displays desirable emission. The sought after redox-mediated off/on fluorescence switching is observed in dichloromethane and toluene solvents.

Electrochemical Properties. In order to verify the electrochemical reversibility of **H_2B-Q**, cyclic voltammetry was employed to measure the redox characteristics of **H_2B-Q**. **H_2B-Q** (0.7 mM) was dissolved in argon-sparged 10% v/v acetonitrile in toluene solution with 0.1 M tetrabutylammonium hexafluorophosphate as the supporting electrolyte. The Ferrocenium/Ferrocene (Fc^+/Fc) redox couple was used to calibrate the silver/silver chloride reference electrode used. The cyclic voltammogram of **H_2B-Q** over 6 scans is shown in Figure 1. Two separate and reversible one electron redox processes

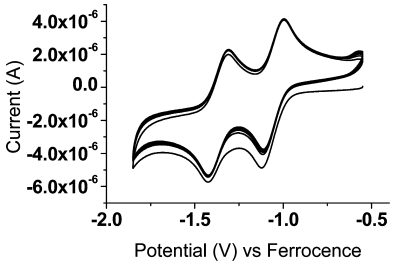

Figure 1. Cyclic Voltammogram of **H_2B-Q** (0.7 mM) dissolved in 10% v/v MeCN in Toluene (0.1 M tetrabutylammonium hexafluorophosphate) under argon recorded at 100 mVs^{-1}. Potentials were normalized to the ferrocene oxidation in these conditions.

were observed, in line with the electrochemical behavior of quinones in aprotic media.[35] The first redox process corresponds to the reduction of **H_2B-Q** to its semiquinone radical form and occurs at −1.05 V (vs ferrocene), in accordance with reported values for ubiquinone (−1.1 V vs ferrocene in DMF).[36] The second process is the subsequent reduction of the semiquinone radical to **H_2B-Q^{2-}** (deprotonated **H_2B-QH_2**) at −1.37 V (vs ferrocene), at more positive bias than what has been reported for ubiquinone (−1.8 V vs ferrocene in DMF, no isoprenoid tail).[36] We attribute an easier (less negative) second reduction to the conjugation of the quinone moiety to the BODIPY core. The radical dianion formed after two subsequent reductions is stabilized via resonance through the BODIPY core, effectively facilitating the second reduction of the quinone moiety. The peak current ratios (i_{pa}/i_{pc}) were estimated to be around 0.93 each, approximately unity, indicating that the radical anion and

DOI: 10.1021/jacs.6b06899
J. Am. Chem. Soc. 2016, 138, 11327−11334

dianion were stable and that no additional reactions took place. Sequential reduction/oxidation over 6 scans were performed to show the high electrochemical reversibility of H_2B-Q and hence its potential utility as a redox-reversible probe.

Redox Reversibility. After demonstrating the electrochemical reversibility of H_2B-Q, we next sought to test the chemical reversibility of the H_2B-Q/H_2B-QH_2 redox couple by taking advantage of the differential fluorescence of the two redox states. The chemical reversibility of the redox couple was evaluated by the one pot sequential reduction of H_2B-Q by sodium borohydride ($NaBH_4$), followed by oxidation of the resulting H_2B-QH_2 by the stable free radical TEMPO (Scheme 3).

Scheme 3. One Pot Reduction and Subsequent Oxidation of H_2BQ

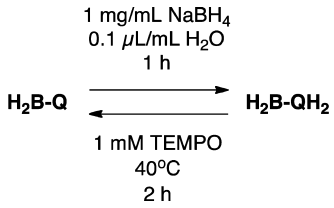

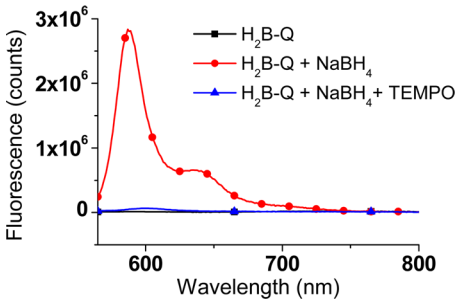

Figure 2. Emission spectra of H_2B-Q (1.3 μM in toluene) before the redox cycle (black, ■), after reduction by sodium borohydride (red, ●), and after subsequent TEMPO oxidation (blue, ▲).

The fluorescence spectra of the starting solution of H_2B-Q, 1.3 μM in toluene, and those following chemical reduction and oxidation are shown in Figure 2. In a cuvette, H_2B-Q was reduced at room temperature over $NaBH_4$ (1 mg/mL) with the addition of a small amount of water (1 μL/mL), acting as a source of protons, to accelerate the reaction. The increasing fluorescence intensity was periodically monitored to determine reaction completion. Maximal fluorescence was observed after 80 min (Figure 2, red trace), at which point the insoluble $NaBH_4$ was filtered out. The spectroscopic properties of the reduction product matched those of isolated H_2B-QH_2, confirming the product of hydride reduction. Significantly, a 200-fold fluorescence enhancement was measured following completion of the reduction reaction, demonstrating the remarkable on/off fluorescence ratio of the probe.

Following confirmation of the reduction product, the resulting H_2B-QH_2 was next oxidized by adding 1 mM TEMPO to the same cuvette. TEMPO aerobic oxidation[37] was used to reconvert H_2B-QH_2 to the initial dark H_2B-Q state. The minimum fluorescence intensity was observed after 2.5 h at 40 °C. The absorption of the solution at this point matched that of pristine H_2B-Q confirming the success of the oxidation. We estimate an overall yield of 52% for the full chemical reduction/oxidation cycle by comparing the initial and final absorbances at 640 nm, where the contribution of H_2B-QH_2 and TEMPO is negligible (Figure S4). At the end of the oxidation, a residual fluorescence was observed with a peak at 606 nm (opposed to 595 nm for H_2B-QH_2), which we attribute to side products from the TEMPO oxidation reaction.

ROS Scavenging and Synergy with α-Tocopherol. To investigate the antioxidant activity of H_2B-QH_2, we next determined the stoichiometric coefficient "*n*" for peroxyl radical scavenging by H_2B-QH_2, that is the number of equivalents of ROS each equivalent of antioxidant may react with. Lipophilic peroxyl radicals were generated via thermolysis of the azo initiator, 2,2′-azobis(4-methoxy-2,4-dimethyl valeronitrile) (MeO-AMVN), in air-equilibrated dichloromethane (eq 1). Intensity-time trajectories were recorded and showed the oxidation of H_2B-QH_2 (as indicated by a drop in fluorescence) over time via reaction with radicals produced upon MeO-AMVN thermolysis (Figure 3, solid red trace). The

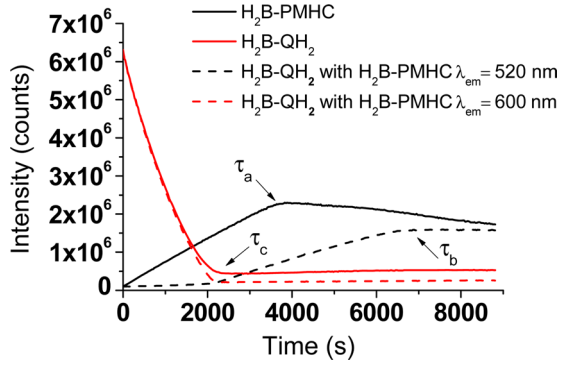

Figure 3. Fluorescence-time trajectories of 100 μM H_2B-PMHC (black traces) or 100 μM H_2B-QH_2 (red traces) in the presence of 0.5 mM MeO-AMVN. Dashed lines indicate the solution where H_2B-PMHC and H_2B-QH_2 were mixed together. H_2B-PMHC was excited at 480 nm and emission was monitored at 520 nm. In turn H_2B-QH_2 was excited at 550 nm and emission was monitored at 600 nm. τ indicates the time of consumption of antioxidant in solution. τ_a = 3670 s (consumption of H_2B-PMHC), τ_b = 6290 s (consumption of H_2B-PMHC in the presence of H_2B-QH_2), and τ_c = 1560 s (consumption of H_2B-QH_2).

fluorescence quenching observed is consistent with the activation of the intramolecular PeT process upon the scavenging of peroxyl radicals and concomitant oxidation of the dihydroquinone moiety (H_2B-QH_2) to the quinone form (H_2B-Q) (eqs 2 and 3). We also note that partial oxidation to the semiquinone radical (eq 2) would lead to the formation of a nonemissive product due to paramagnetic quenching by the unpaired electron.[38]

$$R{-}N{=}N{-}R \xrightarrow{\Delta} \xrightarrow{O_2} 2ROO^{\bullet} + N_2 \quad (1)$$

$$\mathbf{H_2B\text{-}QH_2} + ROO^{\bullet} \rightarrow \mathbf{H_2B\text{-}QH^{\bullet}} + ROOH \quad (2)$$

$$\mathbf{H_2B\text{-}QH^{\bullet}} + ROO^{\bullet} \rightarrow \mathbf{H_2B\text{-}Q} + ROOH \quad (3)$$

The value of *n* was estimated from the consumption time (or inhibition time, τ) observed for H_2B-QH_2 and from the rate of generation of radicals (R_g) upon rearrangement of eq 4. Inhibition times (τ, Figure 3) were determined from the intercept of tangential lines from the increase (or decrease) in fluorescence intensity and the subsequent linear change arising from BODIPY degradation.[21] The rate of generation of free

DOI: 10.1021/jacs.6b06899
J. Am. Chem. Soc. 2016, 138, 11327−11334

radicals (R_g) was in turn estimated from the thermolysis rate constant of the radical initiator (k_i) and the escape fraction (e) from geminate recombination (eq 5).[39] Under the conditions used herein, 0.5 mM MeO-AMVN at 37 °C in air, peroxyl radicals were generated at a constant rate of $R_g = 4.3 \times 10^{-8}$ Ms^{-1} assuming $e = 0.8$ as reported in chloroform.[40,41]

H_2B-QH$_2$ may react with at most 2 equiv of ROS as shown in eqs 2 and 3; however, hydroquinones may have n values ranging from 0 to 2 depending on the reaction conditions, due to their susceptibility to auto-oxidation. Under the conditions we used, we estimated n for **H_2B-QH$_2$** to be 0.7 based on τ_c of 1560 s. Since **H_2B-QH$_2$** requires only 1 reaction with ROS before becoming nonfluorescent the value of $n = 0.7$ obtained thus corresponds to the first oxidation process (formation of the quenched semiquinone, eq 2). This value thus reports partial oxidation and does not reflect the potential reactivity of the semiquinone product or **H_2B-QH$_2$** as a whole.

$$\tau = \frac{n[\text{Antioxidant}]}{R_g} \tag{4}$$

$$R_g = 2ek_i[\text{azo initiator}] \tag{5}$$

Ubiquinone has been noted to participate synergistically with α-tocopherol in the inhibition of lipid peroxidation.[8,42] Specifically it has been shown that upon the scavenging of ROS in lipid membranes by α-tocopherol to yield tocopheroxyl radical, ubiquinol can (in addition to directly scavenging ROS) regenerate α-tocopherol thus prolonging the life of α-tocopherol to act as an antioxidant (Scheme 4). Indeed, in

Scheme 4. Regeneration of α-Tocopherol from the Tocopheroxyl Radical by H_2B-QH$_2$

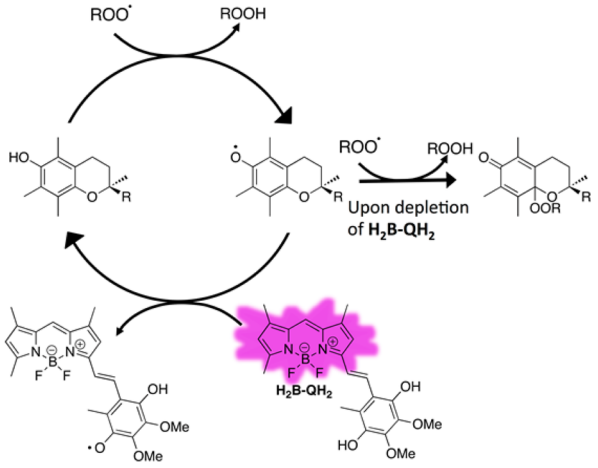

organic solution, ubiquinol reacts with tocopheroxyl radicals very efficiently with a rate constant of about 10^6 M^{-1} s^{-1}, while reaction with peroxyl radicals proceeds with a rate constant of about 10^5 M^{-1} s^{-1} (about 1 order of magnitude slower that that reported for α-tocopherol scavenging of peroxyl radicals).[43] The synergistic regeneration of α-tocopherol by ubiquinol may be understood thermodynamically since the one-electron redox potential of the semiquinone radical/ubiquinol couple is 0.200 V (vs SHE) while that of tocopheroxyl radical/α-tocopherol couple is more positive at 0.50 V (vs SHE), suggesting that ubiquinol will spontaneously reduce the tocopheroxyl radical.[44] Moreover, α-tocopherol has been shown to suppress the rate of auto-oxidation of ubiquinol.[8]

To test the cooperative relationship of **H_2B-QH$_2$** and α-tocopherol, we determined the inhibition time for the oxidation of an α-tocopherol analogue in the presence of **H_2B-QH$_2$**. Specifically, we measured how the presence **H_2B-QH$_2$** delays the formation of chromanone following reaction of two peroxyl radicals with the chromanol moiety. To that effect we utilized **H_2B-PMHC**, a fluorogenic α-tocopherol analogue previously reported by us.[21] **H_2B-PMHC** bears a BODIPY reporter segment and a chromanol (the active part of α-tocopherol) trap segment. In its reduced form, **H_2B-PMHC** is quenched through intramolecular PeT. Oxidation of the nonemissive chromanol by 2 equiv of ROS, via the also nonemissive chromanoxyl radical intermediate yields an emissive chromanone with a distinct spectral window compared to **H_2B-QH$_2$**. By following the onset of enhancement of oxidized **H_2B-PMHC** (establish the inhibition time) in the absence and presence of **H_2B-QH$_2$** we were able to confirm the regeneration of the chromanol form from the chromanoxyl radical by **H_2B-QH$_2$**.

Consistent with a cooperative behavior between **H_2B-QH$_2$** and α-tocopherol, addition of **H_2B-QH$_2$** lead to an induction in the onset of emission from oxidized **H_2B-PMHC** (compare solid vs dashed black traces in Figure 3). Only after full consumption of **H_2B-QH$_2$** (loss of emission from this substrate) did the onset of emission from oxidized **H_2B-PMHC** take place (compare red and black dashed traces in Figure 3). The rate of consumption of **H_2B-QH$_2$** in turn was not affected by the presence of the α-tocopherol analogue. Altogether these results are in accordance with the regeneration of the nonemissive **H_2B-PMHC** from the nonemissive tocopheroxyl radical by **H_2B-QH$_2$**, on par with the reported synergy between α-tocopherol and ubiquinol.[45,46]

Importantly, evaluation of the initial rates of intensity enhancement for **H_2B-PMHC** recorded without vs with **H_2B-QH$_2$** in otherwise identical conditions enabled determining the effect of **H_2B-QH$_2$** on the rate of consumption of **H_2B-PMHC**. On the basis of initial slopes, the rate of consumption of **H_2B-PMHC** (formation of chromanone) was 14-fold slower in the presence of **H_2B-QH$_2$**. Close inspection of Figure 3 further reveals that upon consumption of **H_2B-QH$_2$** the rate of intensity enhancement upon formation of oxidized **H_2B-PMHC** is half that recorded when no **H_2B-QH$_2$** is present in solution This would be consistent with the newly generated ubiquinol semiquinone radical, **H_2B-QH$^\bullet$** from **H_2B-QH$_2$** effectively competing with the α-tocopherol analogue for peroxyl radicals (compare τ_a vs the time span between τ_c and τ_b). A kinetic analysis based on eq 6, where I_∞, I_t, and I_0 are the intensity of **H_2B-PMHC** at the maximum, time t, and at $t = 0$ s, respectively,[21] provides the relative peroxyl radical scavenging activity of **H_2B-QH$^\bullet$** to **H_2B-PMHC**. We obtained a relative rate constant for reaction with peroxyl radicals of 1 for **H_2B-QH$^\bullet$** compared to **H_2B-PMHC** (Figure S5)

$$-\ln\left(\frac{I_\infty - I_t}{I_\infty - I_0}\right) = -\frac{k_{inh}^{\text{H2B-PMHC}}}{k_{inh}^{\text{unk}}}\ln\left(1 - \frac{t}{\tau}\right) \tag{6}$$

Taken together, **H_2B-QH$_2$** reactivity toward α-tocopheroxyl radical is analogous to that reported in the literature for ubiquinol.[8] **H_2B-QH$_2$** can scavenge ROS, as well as inhibit the oxidation of and regenerate α-tocopherol from the tocopheroxyl radical. We have shown this behavior via a drop in fluorescence of **H_2B-QH$_2$** in the presence of **H_2B-PMHC**, as well as via a delayed fluorescence enhancement of **H_2B-PMHC**.

DOI: 10.1021/jacs.6b06899
J. Am. Chem. Soc. 2016, 138, 11327−11334

CONCLUSION

Here we provide guiding rules for the synthesis of a fluorogenic ubiquinone analogue which may provide useful in preparing related analogues in the future. Upon exploiting PeT from BODIPY to the quinone moiety (BODIPY photoinduced oxidation), we have successfully achieved a sensitive probe that is nonemissive when in its oxidized form, yet emissive once the quinone moiety becomes a dihydroquinone. While a current limitation of our newly prepared compound lies in its lower sensitivity in high polarity solvents, an outcome that is related to the extent that PeT may occur from the ubiquinol moiety to the BODIPY dye, we anticipate that future evolutions may drastically enhance the sensitivity at this end of the solvent spectrum. In this regard we further note that a judicious choice of the BODIPY dye utilized may render the oxidized form emissive while the reduced form may in turn be rendered nonemissive.

Important to our work is the preparation route for the ubiquinone analogue that circumvents the synthetic challenges of working with either dihydroquinone or quinone moieties by introducing this functionality through a selective oxidation of a phenol precursor in the last reaction step. Such a protocol should become important in planning related probes with sensitive receptor segments in the future.

The newly developed probe exhibits both chemical and electrochemical reversibility, crucial for monitoring both reduction and oxidation reactions. In addition we show the antioxidant behavior of **H_2B-QH_2**, as well as its synergistic activity with chromanol (the active segment of Vitamin E) toward peroxyl radical scavenging. These are well-established behaviors for ubiquinone which further validates **H_2B-Q** as a suitable fluorogenic analogue of ubiquinone. The newly prepared fluorogenic ubiquinone analogue **H_2B-Q** should provide a crucial tool toward understanding the complex role of ubiquinone in its triple character as an electron and proton couple transporter, and as an antioxidant. We anticipate that **H_2B-Q**/**H_2B-QH_2** may serve as a candidate for understanding complex redox reactions in nonpolar media, and as a model for developing second generation probes with the required sensitivity to monitoring electron transfer processes in mitochondria.

EXPERIMENTAL SECTION

Materials. 8-Acetoxymethyl-2,6-diethyl-1,3,5,7-tetramethyl-pyrromethene fluoroborate (PM605) was purchased from Exciton, Inc. (Dayton, OH). HPLC grade solvents for spectroscopy and column chromatography were purchased through Fisher Scientific. All other chemicals were supplied by Sigma-Aldrich, Co. and used without further purification.

Instrumentation. Absorption spectra were recorded using a Hitachi U-2800 UV−vis−NIR spectrophotometer. Luminescence spectra were recorded using a PTI QuantaMaster spectrofluorimeter using 1 cm × 1 cm quartz cuvettes. Spectra were corrected for detector sensitivity. ^{1}H NMR and ^{13}C NMR spectra were recorded on a Varian VNMRS 500 instrument at 500 and 125 MHz, respectively. Electrospray ionization (ESI) mass spectra were measured on a Bruker maXis impact. Voltammetry experiments were conducted with a computer-controlled CHI760C potentiostat.

Computational Methods. Quantum mechanical calculations were performed using the Gaussian 09 M package.[27] HOMO and LUMO orbital energies were determined from molecular geometries optimized at the B3LYP 6-31G(d) level with an applied polarizable continuum model solvation of toluene. Orbitals were visualized using the Gaussview 5 package.

Fluorescence Quantum Yield. Fluorescence quantum yields were measured using PM605 in acetonitrile as a reference (Φ = 0.72). Absorption and emission spectra of PM605 and the dye of interest were measured -at the same wavelength in each case- in acetonitrile at five different concentrations. The integrated intensity versus absorbance were then plotted and fitted linearly. Relative quantum yields of fluorescence for the unknown with respect to the standard were obtained from eq 7, where Φ, Δ, and n refer, respectively, to the fluorescence quantum yield, the slope obtained from the above-mentioned plot, and the solvent refractive index for the unknown (x) or standard (st).

$$\phi_x = \left(\frac{\Delta_x}{\Delta_{st}}\right) \times \left(\frac{\eta_x^2}{\eta_{st}^2}\right) \tag{7}$$

Fluorescence Lifetime Studies. The fluorescence lifetime measurements were carried out using a Picoquant Fluotime 200 Time Correlated Single Photon Counting (TCSPC) setup employing an LDH 470 diode laser from Picoquant as the excitation source. The laser output was 466 nm. The excitation rate was 10 MHz, and the laser power was adjusted to ensure that the detection frequency was less than 100 kHz. The laser was controlled by a PDL 800 B picosecond laser driver from Picoquant. Photons were collected at the magic angle to mitigate polarization effects.

Electrochemical Studies. Electrochemical measurements were performed using a three-electrode system. The working electrode was a Pt wire. A twisted Pt wire was used as the counter electrode, and a Ag/AgCl electrode (solution of 1 M KCl in a separate fritted compartment) was used as the reference. A 0.1 M solution of tetrabutylammonium hexafluorophosphate in dry acetonitrile/toluene was used as the electrolyte solvent in which 0.7 mM **H_2B-Q** was dissolved. **H_2B-Q** concentrations were determined from the absorption and calculated extinction coefficient. Solutions also contained 1 mM ferrocene as an internal standard. The solution was equilibrated with argon, and measured under inert atmosphere, with a minimum scan rate of 0.1 V s^{-1}. Formal redox potentials were calculated as the average of the cathodic and anodic peak potentials observed in the cyclic voltammograms. All values were reported vs ferrocene.

Kinetic Studies in the Presence of ROS and H_2B-PMHC. Oxidation of **H_2B-QH_2** (100 μM) and/or **H_2B-PMHC** (100 μM) in the presence of peroxyl radicals generated upon MeO-AMVN (0.5 mM) thermolysis was monitored via fluorescence at 37 °C in dichloromethane. Intensity-time trajectories were recorded using a PTI QuantaMaster spectrofluorimeter equipped with a four-position Peltier with motorized turret. Three samples in total were measured (1) **H_2B-QH_2** (100 μM), (2) **H_2B-PMHC** (100 μM), and (3) **H_2B-QH_2** (100 μM) in the presence of **H_2B-PMHC** (100 μM). Samples (1.5 mL) were measured in triangular quartz cuvettes (1 cm × 1 cm) with Teflon stoppers. Each sample was excited at 480 nm (**H_2B-PMHC**) and 550 nm (**H_2B-QH_2**), and emission was collected at 520 nm, and 600 nm respectively over 8000 s. Slits were set to 1 nm spectral resolution.

Synthesis. *6-Methyl-2,3,4-trimethoxy-benzaldehyde*[28] *and 3,5,7-tetramethyl-8-H-pyrromethene fluoroborate (**5**)*[31] were prepared according to literature procedures where spectroscopic data matched those of the reported materials.

*3,4-Dimethoxy-2-hydroxy-6-methylbenzaldehyde (**2**).* 6-Methyl-2,3,4-trimethoxy-benzaldehyde (1.15 g, 5.5 mmol, 1 equiv) was dissolved in dry dichloromethane (36 mL) under argon and cooled to −78 °C using a dry ice-acetone bath. Borontribromide 1 M in dichloromethane solution (4.7 mL, 4.7 mmol, 0.85 equiv) was added dropwise to the reaction mixture. The reaction mixture was gradually warmed up to room temperature. The reaction was monitored by TLC, and it was complete after 2 h. The reaction was quenched with water (30 mL) and extracted 3 times with dichloromethane. The organic phase was washed with brine and dried over anhydrous $MgSO_4$. The solvent was removed under reduced pressure leaving a pale brown solid. The solid residue was loaded onto a silica gel flash column and eluted with hexanes/ethyl acetate 4/1 to give the product

DOI: 10.1021/jacs.6b06899
J. Am. Chem. Soc. 2016, 138, 11327−11334

as a pale yellow solid (1.02 g, 5.2 mmol, 96%). ^{1}H NMR (300 MHz; $CDCl_3$): δ 12.14 (s, 1H), 10.03 (s, 1H), 6.25 (s, 1H), 3.86 (s, 3H), 3.79 (s, 3H), 2.48 (s, 3H). ^{13}C NMR (75 MHz, $CDCl_3$): δ 193.7, 159.0, 157.5, 139.0, 134.4, 114.1, 106.1, 60.7, 56.1, 18.2. HRMS (APCI) for $C_{10}H_{11}O_4$ (M-H) calculated: 195.06628, found 195.06583.

*3-(2-(E)-Vinyl-5,6-dimethoxy-3-methylphenol)-1,5,7-tetramethyl-8-H-pyrromethene fluoroborate (**H$_2$B-phenol**).* Compound **5** (1,3,5,7-Tetramethyl-8-*H*-pyrromethene fluoroborate) (390 mg, 16 mmol, 1 equiv) and **2**(280 mg, 14 mmol, 0.9 equiv) were dissolved in 15 mL toluene under argon. 4-methylpiperidine (0.8 mL) and glacial acetic acid (0.8 mL) were added dropwise to the solution at room temperature. The reaction mixture was stirred for 5 h at 110 °C using a Dean−Stark trap. The reaction mixture was diluted with ethyl acetate, washed once with saturated aqueous $NaHCO_3$, once with saturated aqueous NH_4Cl, and the organic layer was dried over anhydrous $MgSO_4$. The solvent was removed under reduced pressure leaving a dark purple residue. The crude product was loaded onto a silica gel flash column and eluted with hexanes/ethyl acetate 3/2 affording the product as a purple solid (165 mg, 24%). ^{1}H NMR (500 MHz; $CDCl_3$): δ 7.94 (d, J = 16.5 Hz, 1H), 7.43 (d, J = 16.4 Hz, 1H), 6.99 (s, 1H), 6.69 (s, 1H), 6.54 (s, 1H), 6.34 (s, 1H), 6.04 (s, 1H), 3.88 (s, 3H), 3.88 (s, 3H), 2.56 (s, 3H), 2.44 (s, 3H), 2.29 (s, 3H), 2.25 (s, 3H). ^{13}C NMR (126 MHz, $CDCl_3$): δ 156.1, 155.4, 151.7, 149.2, 140.6, 139.7, 135.1, 133.9, 133.6, 133.4, 131.0, 121.6, 118.6, 118.0, 115.7, 115.0, 115.0, 106.2, 61.1, 55.7, 21.3, 14.8, 11.4, 11.3. HRMS (ESI) for $C_{23}H_{24}N_2O_3BF_2$ (M^-) calculated: 425.18535, found: 425.18524.

*3-(2-(E)-Vinyl-5,6-dimethoxy-3-methyl-1,4-quinone)-1,5,7-tetramethyl-8-H-pyrromethene fluoroborate (**H$_2$B-Q**).* Compound **H$_2$B-phenol** (3-(2-(*E*)-Vinyl-5,6-dimethoxy-3-methylphenol)-1,5,7-tetramethyl-8-*H*-pyrromethene fluoroborate) (48 mg, 0.11 mmol, 1 equiv) was dissolved in dry acetonitrile (8 mL). Salcomine (7 mg, 0.02 mmol, 0.2 equiv) was added and the reaction mixture was stirred under an oxygen atmosphere for 3 h. The reaction mixture was filtered through Celite, and the solvent was removed under reduced pressure. The resulting dark purple residue was loaded onto a silica gel flash column and eluted with hexanes/ethyl acetate 3/2 to afford the product as a dark purple residue (22 mg, 45%). ^{1}H NMR (500 MHz; $CDCl_3$): δ 7.69 (d, J = 16.8 Hz, 1H), 7.24 (d, J = 16.8 Hz, 1H), 7.07 (s, 1H), 6.71 (s, 1H), 6.12 (s, 1H), 4.03 (s, 3H), 4.01 (s, 3H), 2.57 (s, 3H), 2.30 (s, 3H), 2.28 (s, 3H), 2.28 (s, 3H). ^{13}C NMR (126 MHz; $CDCl_3$): δ 184.0, 183.6, 160.2, 151.3, 145.1, 144.0, 143.1, 139.4, 138.4, 136.4, 135.3, 134.8, 129.9, 125.6, 120.4, 119.6, 115.6, 61.28, 61.13, 15.1, 13.4, 11.40, 11.30. HRMS (ESI) for $C_{23}H_{24}N_2O_4BF_2$ (M^+) calculated: 441.17917, found: 441.17960.

*3-(2-(E)-Vinyl-5,6-dimethoxy-3-methyl-1,4-quinol)-1,5,7-tetramethyl-8-H-pyrromethene fluoroborate (**H$_2$B-QH$_2$**).* Compound **H$_2$B-Q** (3-(2-(*E*)-Vinyl-5,6-dimethoxy-3-methyl-1,4-quinone)-1,5,7-tetramethyl-8-*H*-pyrromethene fluoroborate) (22 mg, 0.05 mmol, 1 equiv) was dissolved in tetrahydrofuran (1 mL) and methanol (2 mL) under argon. Palladium on carbon (2 mg, 10% by weight) was added followed by the addition of cyclohexene (1 mL). The reaction mixture was heated to 45 °C and stirred for 18 h. It was subsequently filtered through Celite and the solvent was removed under reduced pressure. The resulting crude purple residue was loaded onto a silica gel flash column and eluted with hexanes/ethyl acetate 3/2 to afford the product as a purple residue. ^{1}H NMR (500 MHz; $CDCl_3$): δ 7.94 (d, J = 16.5 Hz, 1H), 7.41 (d, J = 16.5 Hz, 1H), 7.01 (s, 1H), 6.70 (s, 1H), 6.05 (s, 1H), 6.03 (s, 1H), 5.40 (s, 1H), 3.95 (s, 3H), 3.89 (s, 3H), 2.55 (s, 3H), 2.33 (s, 3H), 2.30 (s, 3H), 2.25 (s, 3H). ^{13}C NMR (126 MHz; $CDCl_3$): δ 156.0, 155.4, 142.3, 140.5, 140.18, 140.08, 139.2, 136.8, 135.0, 133.6, 130.6, 123.4, 118.8, 118.36, 118.19, 117.9, 115.1, 60.92, 60.81, 14.8, 12.1, 11.36, 11.31. HRMS (ESI) for $C_{23}H_{24}N_2O_4BF_2$ (M^-) calculated: 441.18027, found: 441.18103.

■ ASSOCIATED CONTENT

Supporting Information

The Supporting Information is available free of charge on the ACS Publications website at DOI: 10.1021/jacs.6b06899.

^{1}H NMR and ^{13}C NMR spectra for compounds **2**, **H$_2$B-phenol**, **H$_2$B-Q**, and **H$_2$B-QH$_2$**. Also UV−vis absorption spectra for compounds **H$_2$B-phenol**, **H$_2$B-Q**, and **H$_2$B-QH$_2$**. Calculated energies of orbitals for **H$_2$B-Q** and **H$_2$B-QH$_2$**.Visualization of calculated orbitals for **H$_2$B-Q** and **H$_2$B-QH$_2$** Absorbance spectra of **H$_2$B-Q** before reduction, after reduction, and after-reoxidation. (PDF)

■ AUTHOR INFORMATION

Corresponding Author

*gonzalo.cosa@mcgill.ca

Notes

The authors declare no competing financial interest.

■ ACKNOWLEDGMENTS

G.C. is grateful to the Natural Sciences and Engineering Research Council of Canada (NSERC) and the Canadian Foundation for Innovation (CFI) for funding; L.E.G. is thankful to Vanier Canada for a postgraduate scholarship; R.G. is thankful to NSERC for a postgraduate scholarship. We are grateful to Richard Lincoln for his help running the DFT calculations presented in the SI of this work.

■ REFERENCES

(1) Scheffler, I. E. In *Mitochondria*; John Wiley & Sons, Inc., 2002; p 141.
(2) Trumpower, B. *J. Bioenerg. Biomembr.* **1981**, *13*, 1.
(3) Echtay, K. S.; Winkler, E.; Klingenberg, M. *Nature* **2000**, *408*, 609.
(4) Rokitskaya, T. I.; Murphy, M. P.; Skulachev, V. P.; Antonenko, Y. N. *Bioelectrochemistry* **2016**, *111*, 23.
(5) Tessensohn, M. E.; Hirao, H.; Webster, R. D. *J. Phys. Chem. C* **2013**, *117*, 1081.
(6) Bonin, J.; Robert, M. *Photochem. Photobiol.* **2011**, *87*, 1190.
(7) Kelso, G. F.; Porteous, C. M.; Coulter, C. V.; Hughes, G.; Porteous, W. K.; Ledgerwood, E. C.; Smith, R. A. J.; Murphy, M. P. *J. Biol. Chem.* **2001**, *276*, 4588.
(8) Shi, H.; Noguchi, N.; Niki, E. *Free Radical Biol. Med.* **1999**, *27*, 334.
(9) Schnurr, K.; Hellwing, M.; Seidemann, B.; Jungblut, P.; Kühn, H.; Rapoport, S. M.; Schewe, T. *Free Radical Biol. Med.* **1996**, *20*, 11.
(10) Desbats, M. A.; Vetro, A.; Limongelli, I.; Lunardi, G.; Casarin, A.; Doimo, M.; Spinazzi, M.; Angelini, C.; Cenacchi, G.; Burlina, A.; Rodriguez Hernandez, M. A.; Chiandetti, L.; Clementi, M.; Trevisson, E.; Navas, P.; Zuffardi, O.; Salviati, L. *Eur. J. Hum. Genet.* **2015**, *23*, 1254.
(11) Wang, Y.; Oxer, D.; Hekimi, S. *Nat. Commun.* **2015**, *6*, 6393.
(12) Ogasahara, S.; Engel, A. G.; Frens, D.; Mack, D. *Proc. Natl. Acad. Sci. U. S. A.* **1989**, *86*, 2379.
(13) Kelso, G. F.; Porteous, C. M.; Coulter, C. V.; Hughes, G.; Porteous, W. K.; Ledgerwood, E. C.; Smith, R. A.; Murphy, M. P. *J. Biol. Chem.* **2001**, *276*, 4588.
(14) Dare, A. J.; Bolton, E. A.; Pettigrew, G. J.; Bradley, J. A.; Saeb-Parsy, K.; Murphy, M. P. *Redox Biol.* **2015**, *5*, 163.
(15) Coudray, C.; Fouret, G.; Lambert, K.; Ferreri, C.; Rieusset, J.; Blachnio-Zabielska, A.; Lecomte, J.; Ebabe Elle, R.; Badia, E.; Murphy, M. P.; Feillet-Coudray, C. *Br. J. Nutr.* **2016**, *115*, 1155.
(16) Komatsu, H.; Shindo, Y.; Oka, K.; Hill, J. P.; Ariga, K. *Angew. Chem., Int. Ed.* **2014**, *53*, 3993.
(17) Ma, W.; Qin, L.-X.; Liu, F.-T.; Gu, Z.; Wang, J.; Pan, Z. G.; James, T. D.; Long, Y.-T. *Sci. Rep.* **2013**, *3*, 3.
(18) Silvers, W. C.; Prasai, B.; Burk, D. H.; Brown, M. L.; McCarley, R. L. *J. Am. Chem. Soc.* **2013**, *135*, 309.
(19) Oleynik, P.; Ishihara, Y.; Cosa, G. *J. Am. Chem. Soc.* **2007**, *129*, 1842.
(20) Liu, X.-Y.; Long, Y.-T.; Tian, H. *RSC Adv.* **2015**, *5*, 57263.

DOI: 10.1021/jacs.6b06899
J. Am. Chem. Soc. 2016, 138, 11327−11334

(21) Krumova, K.; Friedland, S.; Cosa, G. *J. Am. Chem. Soc.* **2012**, *134*, 10102.
(22) Godin, R.; Liu, H.-W.; Smith, L.; Cosa, G. *Langmuir* **2014**, *30*, 11138.
(23) Kowada, T.; Maeda, H.; Kikuchi, K. *Chem. Soc. Rev.* **2015**, *44*, 4953.
(24) Loudet, A.; Burgess, K. *Chem. Rev.* **2007**, *107*, 4891.
(25) Wood, T. E.; Thompson, A. *Chem. Rev.* **2007**, *107*, 1831.
(26) Lincoln, R.; Greene, L. E.; Krumova, K.; Ding, Z.; Cosa, G. *J. Phys. Chem. A* **2014**, *118*, 10622.
(27) Frisch, M. J.; Trucks, G. W.; Schlegel, H. B.; Scuseria, G. E.; Robb, M. A.; Cheeseman, J. R.; Scalmani, G.; Barone, V.; Mennucci, B.; Petersson, G. A.; Nakatsuji, H.; Caricato, M.; Li, X.; Hratchian, H. P.; Izmaylov, A. F.; Bloino, J.; Zheng, G.; Sonnenberg, J. L.; Hada, M.; Ehara, M.; Toyota, K.; Fukuda, R.; Hasegawa, J.; Ishida, M.; Nakajima, T.; Honda, Y.; Kitao, O.; Nakai, H.; Vreven, T.; Montgomery, J. A., Jr.; Peralta, J. E.; Ogliaro, F.; Bearpark, M. J.; Heyd, J.; Brothers, E. N.; Kudin, K. N.; Staroverov, V. N.; Kobayashi, R.; Normand, J.; Raghavachari, K.; Rendell, A. P.; Burant, J. C.; Iyengar, S. S.; Tomasi, J.; Cossi, M.; Rega, N.; Millam, N. J.; Klene, M.; Knox, J. E.; Cross, J. B.; Bakken, V.; Adamo, C.; Jaramillo, J.; Gomperts, R.; Stratmann, R. E.; Yazyev, O.; Austin, A. J.; Cammi, R.; Pomelli, C.; Ochterski, J. W.; Martin, R. L.; Morokuma, K.; Zakrzewski, V. G.; Voth, G. A.; Salvador, P.; Dannenberg, J. J.; Dapprich, S.; Daniels, A. D.; Farkas, Ö.; Foresman, J. B.; Ortiz, J. V.; Cioslowski, J.; Fox, D. J. *Gaussian 09*; Gaussian, Inc.: Wallingford, CT, 2009.
(28) Lipshutz, B. H.; Lower, A.; Berl, V.; Schein, K.; Wetterich, F. *Org. Lett.* **2005**, *7*, 4095.
(29) Schäfer, W. *Chem. Ber.* **1966**, *99*, 160.
(30) Mcomie, J. F. W.; Watts, M. L.; West, D. E. *Tetrahedron* **1968**, *24*, 2289.
(31) Wu, L.; Burgess, K. *Chem. Commun.* **2008**, 4933.
(32) Zhang, X.; Xiao, Y.; Qi, J.; Qu, J.; Kim, B.; Yue, X.; Belfield, K. D. *J. Org. Chem.* **2013**, *78*, 9153.
(33) Ma, W.; Zhou, H.; Ying, Y.-L.; Li, D.-W.; Chen, G.-R.; Long, Y.-T.; Chen, H.-Y. *Tetrahedron* **2011**, *67*, 5990.
(34) Hu, R.; Lager, E.; Aguilar-Aguilar, A.; Liu, J.; Lam, J. W. Y.; Sung, H. H. Y.; Williams, I. D.; Zhong, Y.; Wong, K. S.; Peña-Cabrera, E.; Tang, B. Z. *J. Phys. Chem. C* **2009**, *113*, 15845.
(35) Costentin, C.; Robert, M.; Savéant, J.-M. *Chem. Rev.* **2010**, *110*, PR1.
(36) Dutton, P. L.; Bruce, J. M. *FEBS Lett.* **1983**, *155*, 273.
(37) Studer, A.; Vogler, T. *Synthesis* **2008**, *2008*, 1979.
(38) Turro, N. J.; Ramamurthy, V.; Scaiano, J. C. *Principles of Molecular Photochemistry: An Introduction*; University Science Books: Sausalito, CA, 2009.
(39) Barclay, L. R. C.; Locke, S. J.; MacNeil, J. M.; VanKessel, J.; Burton, G. W.; Ingold, K. U. *J. Am. Chem. Soc.* **1984**, *106*, 2479.
(40) Noguchi, N.; Yamashita, H.; Gotoh, N.; Yamamoto, Y.; Numano, R.; Niki, E. *Free Radical Biol. Med.* **1998**, *24*, 259.
(41) We anticipate that a value of $e = 0.8$ is an underestimate, since this value was determined in chloroform, and our experiments are carried out in dichloromethane. Since geminate recombination is more likely in more viscous solvents, we expect $e > 0.8$ in the dichlromethane (less viscous).
(42) Gille, L.; Rosenau, T.; Kozlov, A. V.; Gregor, W. *Biochem. Pharmacol.* **2008**, *76*, 289.
(43) Kagan, V. E.; Tyurina, Y. Y.; Witt, E. In *Fat-Soluble Vitamins*; Quinn, P. J., Kagan, V. E., Eds.; Springer: Boston, MA, 1998; p 491.
(44) Buettner, G. R. *Arch. Biochem. Biophys.* **1993**, *300*, 535.
(45) Frei, B.; Kim, M. C.; Ames, B. N. *Proc. Natl. Acad. Sci. U. S. A.* **1990**, *87*, 4879.
(46) Ouchi, A.; Nagaoka, S.-i.; Mukai, K. *J. Phys. Chem. B* **2010**, *114*, 6601.

DOI: 10.1021/jacs.6b06899
J. Am. Chem. Soc. 2016, 138, 11327−11334